

## RESONANT NON-LINEAR SPECTROSCOPY IN STRONG FIELDS <sup>☆</sup>

Bernhard DICK <sup>‡</sup> and R.M. HOCHSTRASSER

*Department of Chemistry, University of Pennsylvania, Philadelphia, Pennsylvania 19104, USA*

Received 22 November 1982

A method is presented to describe multiple resonant non-linear spectra in the presence of strong laser fields. The Liouville equation for the density operator of the molecular system is transformed to a time-independent linear equation system. This can be easily solved rigorously by numerical methods or, after partitioning into a strong-field part and a perturbation, the solution can be obtained analytically by a novel perturbative approach. The results account for power broadening, Rabi splitting of signals, and power-induced extra resonances, the latter being related to the pure dephasing-induced resonances in the weak-field limit. The method can be applied to a large number of multiple resonant non-linear spectroscopies, especially CARS, CSRS, coherent Rayleigh scattering and sum- or difference-frequency generation.

### 1. Introduction

In recent years there were many applications of coherent non-linear methods to the study of molecular systems [1]. In a typical experiment a sample is subjected to a number of electromagnetic fields, and harmonics or other combinations of the field frequencies are observed. The intensities of these generated waves are studied as functions of input frequencies. The signal strength at any choice of frequencies is usually measured as a function of the input field intensities so that processes can be associated with specific orders of the susceptibility in the expansion of the macroscopic polarization in powers of the incident field strengths. This same approach is employed in many cases where it is not evident, a priori, that a perturbation expansion of the polarization is meaningful — namely the situation where the incident fields are resonant with strong transitions of the system.

The relationships between the observed coherent spectra and theoretical descriptions of molecular energy levels and their dynamics is usually described by means of an iterative solution of the Liouville equation to yield the reduced density operator, and hence the induced dipole moment of the system, to the required order in incident fields. This approach yields the  $n$ th-order density operator in the form of an  $n$ -tuple time-ordered integral. Such a description leads naturally to time-ordered diagrammatic methods for obtaining the various susceptibilities [2–4]. However not all the diagrams that contribute to a particular process are physically distinguishable so that it is obvious that this time-ordered field approach is not a unique picture of these non-linear processes. The question arises as to whether there is a picture in which the physical response can be considered time independent. Such a result would be analogous to the rotating-frame description of resonant processes in a two-level system [5]. Indeed it was shown by Wilcox and Lamb [6] in relation to microwave and optical double resonance spectroscopy, and by Freed [7] in relation to magnetic resonance phenomena that in certain cases the equation of motion of the state vector for a many-level system driven by a number of fields could be written with time-independent coefficients.

The need for a non-perturbative approach to non-linear optical responses and spectroscopies has sharpened recently because of the increasing importance of multiple resonant phenomena using intense laser fields. It is clear that the response of media to rather strong fields is accurately described by the perturbation approach when the

<sup>☆</sup> This research was supported by an NIH grant (GM12592) and in part by the NSF/MRL Program, under Grant No. DMR-7923647.

<sup>‡</sup> A research Fellowship of the “Deutsche Forschungsgemeinschaft” is gratefully acknowledged.

driving fields are far from resonance such as with second-harmonic generation in transparent media. Even in cases where there is a single resonance at a combination frequency the perturbation approach is valid when the medium is transparent at the incident frequencies unless the light intensities become much higher than are easily obtained with conventional tunable dye lasers. Examples of this would be CARS and two-photon absorption. However when the medium has resonances at the incident frequencies and their combinations it is no longer evident that a third-order non-linear signal can be detected at fields that are weak enough for the perturbation approach to be valid.

Of particular spectroscopic interest are the three- and four-level resonant processes including polarization spectroscopy [8], CARS and CSRS [9–12], coherent Rayleigh processes [12–16], and resonant conjugate wave configurations for spectroscopy [17,18]. In all of these methods the condition of full resonance can be achieved such that each level pair is driven by the incident fields or their combination, or is resonant with the outgoing wave. Recent work from this laboratory has concerned CARS and CSRS processes in four-level systems [10–12]. One of the cases studied was pentacene in benzoic acid [10] which at low temperatures displays sharp line spectra that allow the non-linear signals to be analyzed confidently. There are in these experiments two incident beams having frequencies  $\omega_1$  and  $\omega_2$  such that the  $0-0'$  and  $v-v'$  transitions are near resonant with  $\omega_1$ , a Raman transition is resonant with  $\omega_1 - \omega_2$ , a fluorescence transition  $v-0'$  is resonant with  $\omega_2$ , and the outgoing wave at  $2\omega_1 - \omega_2$  is resonant with the  $0-v'$  transition. We have recently shown that even at low laser powers it was not possible with this system to avoid the occurrence of higher-order processes in resonant  $\chi^{(3)}$  spectroscopy [10]. Furthermore in our earliest study of the pentacene–benzoic-acid mixed crystal [10] we observed severe field broadening of the lines in the CARS spectrum when unattenuated nitrogen-pumped dye lasers were used for the experiments. These field-induced effects require a quantitative description.

The resonant Stokes generation that occurs when two fields are used to drive a four-level system (resonant CSRS) is described by three time-ordered diagrams of the type described above [11]. One of these describes a Raman transition of the ground state and the other two describe an excited-state Raman transition. In the absence of pure dephasing the excited-state Raman transition is not present because of an exact cancellation of this resonant amplitude when both the relevant time-ordered diagrams are considered [11]. In solids, as the temperature is raised, the excited-state resonance appears [11,12] in a process we have termed DICE (dephasing-induced coherent emission). This process we understand to be of similar origin to the PIER-4 process (pressure-induced extra resonances in 4-wave mixing) reported recently for Na vapor [19]. A full understanding of these processes requires careful identification of effects higher order than third in the applied fields. In addition there is the challenge of finding a new picture of these non-linear processes in which the DICE effects appear more naturally, and that displays more clearly the field-intensity effects on the generation of the extra resonances.

## 2. Liouville equations under fully resonant conditions

The coherently generated non-linear signals produced by mixing optical fields in a non-linear medium can be calculated by solving Maxwell's equations with a non-linear polarization obtained from perturbation theory [20] as the source term. This polarization is given in terms of quantum-mechanical matrix elements of the molecular system as

$$P = \text{Tr}(\rho\mu) . \quad (1)$$

Here  $\rho$  denotes the reduced density matrix of the molecular system, and  $\mu$  the dipole operator. The time evolution of  $\rho$  is described by the Liouville equation:

$$\dot{\rho} = i[\rho, H] + (\dot{\rho})^R , \quad (2)$$

where in the Markov approximation, the elements of the damping matrix are given by

$$(\dot{\rho})_{\alpha\alpha}^R = -\Gamma_{\alpha\alpha}\rho_{\alpha\alpha} + \sum_{\beta} \gamma_{\beta\alpha}\rho_{\beta\beta}, \quad (\dot{\rho})_{\alpha\beta}^R = -\Gamma_{\alpha\beta}\rho_{\alpha\beta}. \quad (3)$$

The phenomenological damping parameters describe population decay ( $\Gamma_{\alpha\alpha}$ ), phase relaxation ( $\Gamma_{\alpha\beta}$ ) and feeding ( $\gamma_{\beta\alpha}$ ). Although  $\Gamma_{\alpha\beta} = \Gamma_{\beta\alpha}$ , the feeding matrix is not symmetric because  $\gamma_{\beta\alpha} \neq \gamma_{\alpha\beta}$ . The phase relaxation includes both population decay and a contribution  $\Gamma'_{\alpha\beta}$  called pure dephasing:

$$\Gamma_{\alpha\beta} = \frac{1}{2}(\Gamma_{\alpha\alpha} + \Gamma_{\beta\beta}) + \Gamma'_{\alpha\beta}. \quad (4)$$

The condition  $\text{Tr}(\dot{\rho})^R = 0$  implies that the population decay rates and the feeding constants are related as follows:

$$\Gamma_{\alpha\alpha} = \sum_{\beta} \gamma_{\alpha\beta}. \quad (5)$$

The Hamilton operator  $H$  is the sum of the molecular hamiltonian  $H^0$  and the interaction term  $V$ . In the basis chosen  $H^0$  is diagonal:

$$H_{\mu\nu} = \omega_{\mu} \delta_{\mu\nu}. \quad (6)$$

The additional potential is given in the dipole approximation as

$$V = -\boldsymbol{\mu} \cdot \mathbf{E}(t) \quad (7)$$

and the external applied field is a function with  $2n$  Fourier components:

$$\mathbf{E}(t) = \sum_j^n \mathbf{e}_j [\epsilon_j^* \exp(-i\omega_j t) + \epsilon_j \exp(i\omega_j t)]. \quad (8)$$

In the general case eq. (2) is a system of coupled linear differential equations, which, in the limit of weak fields, may be solved by expanding  $\rho$  in powers of these fields. When the feeding terms are neglected the differential equations for each step of the iteration are decoupled. This is the usual procedure by means of which non-linear susceptibilities are calculated [11,20].

If one or more of the field components in eq. (8) has a large amplitude — a more precise definition of a large amplitude will be given later — an expansion of  $\rho$  in powers of the fields and the iterative solution procedure is not practical. Under fully resonant conditions, however, a transformation can be applied to eq. (2) which removes all terms rapidly varying in time. What remains is a system of equations for the slowly varying envelopes which can be solved both for transient and steady-state effects. The conditions, under which such a transformation is possible, are found to be:

- (i) All fields, applied or generated, must be close to a resonance of the molecular system.
- (ii) Each pair of levels of the molecular system can be driven by no more than one resonant field.
- (iii) The number of externally applied fields must be less than  $N$  for an  $N$ -level system.
- (iv) The externally applied fields may not form a “closed loop” in the level diagram.

The first two conditions lead to important simplifications of the matrix elements of  $V$ . Let  $\mu$  and  $\nu$  be two levels of the system with energy difference  $\omega_{\mu\nu} = \omega_{\mu} - \omega_{\nu}$ , and let the field component close to resonance have frequency  $\omega_j$ . Under such circumstances only the fully resonant contribution resulting from one rotating part of the field  $\epsilon_j$  need be retained and all other contributions neglected in the matrix element  $V_{\mu\nu}$

$$V_{\mu\nu} = -(\boldsymbol{\mu}_{\mu\nu} \cdot \mathbf{e}_j) \epsilon_j \exp(-is_{\mu\nu}\omega_j t),$$

where the factor

$$s_{\mu\nu} = \text{sign}(\omega_{\mu\nu}) \quad (9)$$

ensures that the proper field component is chosen for a rotating-wave approximation. From the same considera-

tions we can show that only one Fourier component for each matrix element of the density operator is needed, namely the one rotating with the frequency of the corresponding near-resonance field:

$$\rho_{\mu\nu} = \tilde{\rho}_{\mu\nu} \exp(-is_{\mu\nu}\omega_j t). \quad (10)$$

The matrix elements of  $\tilde{\rho}$  are then either slowly varying in time or constant.

Now consider the transformation of the density matrix using the unitary operator  $U = e^{iAt}$  where  $A$  is a diagonal matrix having elements  $A_\mu$ . The transformed density operator is

$$(U\rho U^\dagger)_{\mu\nu} = \tilde{\rho}_{\mu\nu} \exp[-i(s_{\mu\nu}\omega_j - A_\mu + A_\nu)t]. \quad (11)$$

The time dependence is removed by choosing the parameters  $A_\mu$  to satisfy

$$\omega_j = s_{\mu\nu}(A_\mu - A_\nu) = |A_\mu - A_\nu|. \quad (12)$$

In an  $N$ -level system  $N(N-1)/2$  equations of the type (12) exist, but only  $N-1$  parameters  $A_\mu$  may be chosen independently. Consequently  $(N-2)(N-1)/2$  additional relations must exist between the field frequencies  $\omega_j$  in order to make eq. (12) valid for all level pairs. This is the source for the conditions (iii) and (iv) listed above.

As an illustration of these conditions consider, as in fig. 1, the general numbering scheme for three- and four-level systems. If  $A_\mu$  is equal to the frequency in resonance with the  $a \rightarrow \mu$  transition, we would have

$$A_a = 0, \quad A_b = \omega_1, \quad A_c = \omega_2, \quad A_d = \omega_4. \quad (13)$$

Consequently eq. (12) would be fulfilled for all matrix elements (11) coupling the initial state with any excited state. For the other matrix elements we obtain the conditions

$$\omega_3 = A_c - A_b = \omega_2 - \omega_1, \quad \omega_5 = A_d - A_b = \omega_4 - \omega_1, \quad \omega_6 = A_d - A_c = \omega_4 - \omega_2. \quad (14)$$

These conditions may be recognized as frequency *selection rules* for the generated waves. If  $\omega_1$  and  $\omega_2$  are the ingoing waves in a three-level system, eq. (14) expresses the fact that we expect  $\rho_{bc}$  to rotate with the difference frequency. Equally, we could take  $\omega_1$  and  $\omega_3$  as ingoing waves and therefore restrict  $\rho_{ac}$  to rotate with the sum frequency, and so on.

The rule (iv) arises because each frequency is used to define a particular level pair, so that a set of frequencies defines a multilevel system. For example,  $\omega_1$  and  $\omega_2$  define a three-level system and  $\omega_3$  adds no new level. The set of frequencies  $\omega_1$ ,  $\omega_2$  and  $\omega_4$  on the other hand defines a four-level problem. In the treatment that follows all field indices are included and the results for different possible ingoing waves may then be obtained by setting the unwanted fields equal to zero.

Having defined the field components in the above manner, the transformation  $U$  will remove all rapidly varying terms in  $\rho$  and  $V$ :

$$U\rho U^\dagger = \tilde{\rho}, \quad UVU^\dagger = \tilde{V}. \quad (15)$$

The matrix elements of  $\tilde{V}$  have the form

$$\tilde{V}_{\mu\nu} = -(\mathbf{u}_{\mu\nu} \cdot \mathbf{e}_j) \epsilon_j = -W_j(\mu \leftarrow \nu), \quad (16)$$

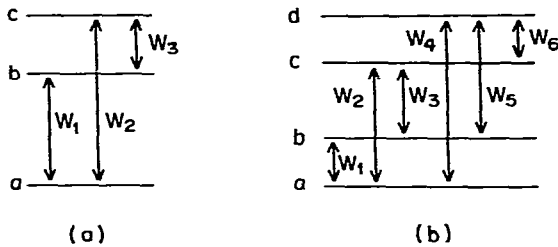


Fig. 1. General numbering scheme for waves and levels in three- and four-level systems under fully resonant conditions.

where the one-photon resonant Rabi frequency is  $W_j$ . Finally, the transformation of the relaxation matrix is obtained by replacing all matrix elements of  $\rho$  in eq. (3) by the corresponding matrix element of  $\tilde{\rho}$ :

$$U(\dot{\rho})^R U^\dagger = (\dot{\tilde{\rho}})^R . \quad (17)$$

The equation of motion for  $\tilde{\rho}$  can now be rewritten in the form

$$\dot{\tilde{\rho}} = -i[\tilde{\rho}, A] + i[\tilde{\rho}, H^0 + \tilde{V}] + (\dot{\tilde{\rho}})^R . \quad (18a)$$

Since  $(\dot{\tilde{\rho}})^R$  is linear in  $\tilde{\rho}$ , eq. (18) can be rearranged into a linear equation system:

$$\dot{\tilde{\rho}} = \mathbf{X} \tilde{\rho} , \quad (18b)$$

where  $\tilde{\rho}$  and  $\dot{\tilde{\rho}}$  are considered to be arranged as column vectors and  $\mathbf{X}$  is a matrix of dimension  $N^2 \times N^2$ .  $\mathbf{X}$  can be regarded as matrix representation of a superoperator, and a generator formula for its matrix elements is given in appendix A. The main point is that  $\mathbf{X}$  is independent of time.

### 3. Solution of the slowly varying Liouville equation

If the field amplitudes of the ingoing waves are essentially constant in the interval  $0 \leq t < \infty$ , eq. (18) can be easily Laplace transformed:

$$sr - \tilde{\rho}_0 = \mathbf{X} \cdot r , \quad (19)$$

where  $\tilde{\rho}_0 = \tilde{\rho}(t=0)$  and  $r$  is the Laplace transform of  $\tilde{\rho}$ :

$$r(s) = \int_0^\infty dt e^{-st} \tilde{\rho}(t) . \quad (20)$$

The system of coupled differential equations is thereby transformed into a linear equation system which can be formally solved in the form

$$r = -(\mathbf{X} - s\mathbf{1})^{-1} \cdot \tilde{\rho}_0 . \quad (21)$$

The back transform of  $r$  finally yields the time evolution of  $\tilde{\rho}$  for fields that are switched on at  $t=0$ . The steady-state result can be directly obtained from

$$\tilde{\rho}(\infty) = \lim_{s \rightarrow 0} (sr) . \quad (22)$$

An alternative way to obtain the steady-state result would be to set  $\dot{\tilde{\rho}}$  in eq. (18) to zero and solve

$$\mathbf{X} \tilde{\rho}(\infty) = 0 . \quad (23)$$

The determinant of  $\mathbf{X}$  vanishes (see appendix B), hence eq. (23) has a non-trivial solution. This is seen by noting that the rows of  $\mathbf{X}$  corresponding to the diagonal elements of  $\tilde{\rho}$  sum up to a zero row since

$$\text{Tr} \dot{\tilde{\rho}} = 0 . \quad (24)$$

We can therefore replace one of these rows, say the first one corresponding to  $\tilde{\rho}_{aa}$ , by the row equivalent to

$$\text{Tr} \tilde{\rho} = 1 , \quad (25)$$

yielding the new matrix equation

$$\mathbf{X}' \tilde{\rho}(\infty) = \mathbf{a} , \quad \mathbf{a} = [1, 0, 0, \dots, 0] , \quad (26)$$

which can formally be solved by matrix inversion of  $\mathbf{X}'$ .

#### 4. Treatment of perturbations

The solution of the equation systems (21) or (26) is possible, but analytically cumbersome, since the matrices to be inverted are of dimension  $9 \times 9$  and  $16 \times 16$  for three-level and four-level systems. However numerical solutions can be readily accomplished in the general case. Frequently situations are encountered where not all of the fields  $\omega_1$ ,  $\omega_2$  and  $\omega_3$  are strong. The matrix relations (21) and (26) can be simplified considerably if not all of the ingoing waves are chosen as strong fields, and the others are treated by a perturbation theory. The analytical results obtained in this way give insight into the effects produced by strong fields in fully resonant non-linear spectroscopy.

It is convenient to subdivide  $\mathbf{X}$  into a strong-field part  $\mathbf{X}^0$  and a perturbation  $\mathbf{W}$ . Such a partitioning is always easily accomplished since  $\mathbf{X}$  is linear in all field amplitudes.  $\mathbf{X}^0$  is obtained by striking out all field elements from  $\mathbf{X}$  that are to be chosen as weak. The remaining terms are incorporated in  $\mathbf{W}$ . Furthermore we expand  $\mathbf{r}$  in powers of the weak-field part:

$$\mathbf{r} = \mathbf{r}^{(0)} + \mathbf{r}^{(1)} + \dots + \mathbf{r}^{(n)} + \dots \quad (27)$$

Introduction of these definitions into eq.(21) yields the "zero-order" result

$$(\mathbf{X}^0 - s\mathbf{1})\mathbf{r}^{(0)} = -\tilde{\mathbf{p}}_0. \quad (28)$$

The higher orders of  $\mathbf{r}$  obey the recurrence relation

$$(\mathbf{X}^0 - s\mathbf{1}) \cdot \mathbf{r}^{(n)} = -\mathbf{W} \cdot \mathbf{r}^{(n-1)}. \quad (29)$$

The first order is found by replacing the vector  $\tilde{\mathbf{p}}_0$  by  $\mathbf{W} \cdot \mathbf{r}^{(0)}$  and solving the same equation system again. The formal solution to (28) and (29) is

$$\mathbf{r}^{(0)} = -(\mathbf{X}^0 - s\mathbf{1})^{-1} \cdot \tilde{\mathbf{p}}_0, \quad \mathbf{r}^{(n)} = [-(\mathbf{X}^0 - s\mathbf{1})^{-1} \cdot \mathbf{W}]^n \cdot \mathbf{r}^{(0)}. \quad (30)$$

The solution of eq.(26) is also straightforward. Instead of inverting  $\mathbf{X}^0 - s\mathbf{1}$  it may be easier to directly solve eq. (29), since the vector  $\mathbf{W} \cdot \mathbf{r}^{(n-1)}$  may contain many zero elements. In the special case that *all* field amplitudes are assumed to be weak the required matrix inversion is easily performed and eq.(30) yields the non-linear susceptibilities under fully resonant conditions that are usually obtained by multiple time integrals [11,20].

#### 5. Application to the three-level system

The explicit form of the linear equation system (18b) for a three-level system is easily found using the matrix elements for the  $\mathbf{X}$ -superoperator from eq. (A2). This matrix equation is displayed below:

$$\begin{bmatrix} -s & \gamma_{ba} & \gamma_{ca} & -iW_1^* & iW_1 & -iW_2^* & 0 & iW_2 & 0 \\ 0 & -\Gamma_{bb}-s & \gamma_{cb} & iW_1^* & -iW_1 & 0 & -iW_3^* & 0 & iW_3 \\ 0 & 0 & -\Gamma_{cc}-s & 0 & 0 & iW_2^* & iW_3^* & -iW_2 & -iW_3 \\ -iW_1 & iW_1 & 0 & -i\Delta_{ab}-s & 0 & -iW_3^* & 0 & 0 & iW_2 \\ iW_1^* & -iW_1^* & 0 & 0 & i\Delta_{ab}^*-s & 0 & -iW_2^* & iW_3 & 0 \\ -iW_2 & 0 & iW_2 & -iW_3 & 0 & -i\Delta_{ac}-s & iW_1 & 0 & 0 \\ 0 & -iW_3 & iW_3 & 0 & -iW_2 & iW_1^* & -i\Delta_{bc}-s & 0 & 0 \\ iW_2^* & 0 & -iW_2^* & 0 & iW_3^* & 0 & 0 & i\Delta_{ac}^*-s & -iW_1^* \\ 0 & iW_3^* & -iW_3^* & iW_2^* & 0 & 0 & 0 & -iW_1 & i\Delta_{bc}^*-s \end{bmatrix} \begin{bmatrix} r_{aa} \\ r_{bb} \\ r_{cc} \\ r_{ab} \\ r_{ba} \\ r_{ac} \\ r_{bc} \\ r_{ca} \\ r_{cb} \end{bmatrix} = - \begin{bmatrix} 1 \\ 0 \\ 0 \\ 0 \\ 0 \\ 0 \\ 0 \\ 0 \\ 0 \end{bmatrix}, \quad (31)$$

where

$$\begin{aligned}\Delta_{ab} &= \omega_1 + \omega_{ab} - i\Gamma_{ab} = -\Delta_{ba}^*, & \Delta_{ac} &= \omega_2 + \omega_{ac} - i\Gamma_{ac} = -\Delta_{ca}^*, \\ \Delta_{bc} &= \omega_3 + \omega_{bc} - i\Gamma_{bc} = -\Delta_{cb}^*,\end{aligned}\quad (32)$$

and

$$W_1 = (\mu_{ab} \cdot e_1) \epsilon_1, \quad W_2 = (\mu_{ac} \cdot e_2) \epsilon_2, \quad W_3 = (\mu_{bc} \cdot e_3) \epsilon_3. \quad (33)$$

For the sake of completeness we give also the equation system for the steady-state result corresponding to eq. (26)

$$\begin{bmatrix} 1 & 1 & 1 & 0 & 0 & 0 & 0 & 0 & 0 & 0 \\ 0 & -\Gamma_{bb} & \gamma_{cb} & iW_1^* & -iW_1 & 0 & -iW_3^* & 0 & iW_3 & 0 \\ 0 & 0 & -\Gamma_{cc} & 0 & 0 & iW_2^* & iW_3^* & -iW_2 & -iW_3 & 0 \\ -iW_1 & iW_1 & 0 & -i\Delta_{ab} & 0 & -iW_3^* & 0 & 0 & iW_2 & 0 \\ iW_1^* & -iW_1^* & 0 & 0 & i\Delta_{ab}^* & 0 & iW_2^* & iW_3 & 0 & 0 \\ -iW_2 & 0 & iW_2 & -iW_3 & 0 & -i\Delta_{ac} & iW_1 & 0 & 0 & 0 \\ 0 & -iW_3 & iW_3 & 0 & -iW_2 & iW_1^* & -i\Delta_{bc} & 0 & 0 & 0 \\ iW_2^* & 0 & -iW_2^* & 0 & iW_3^* & 0 & 0 & i\Delta_{ac}^* & -iW_1^* & 0 \\ 0 & iW_3^* & -iW_3^* & iW_2^* & 0 & 0 & 0 & -iW_1 & i\Delta_{bc}^* & 0 \end{bmatrix} \begin{bmatrix} \tilde{\rho}_{aa} \\ \tilde{\rho}_{bb} \\ \tilde{\rho}_{cc} \\ \tilde{\rho}_{ab} \\ \tilde{\rho}_{ba} \\ \tilde{\rho}_{ac} \\ \tilde{\rho}_{bc} \\ \tilde{\rho}_{ca} \\ \tilde{\rho}_{cb} \end{bmatrix} = \begin{bmatrix} 1 \\ 0 \\ 0 \\ 0 \\ 0 \\ 0 \\ 0 \\ 0 \\ 0 \end{bmatrix}. \quad (34)$$

In both eqs. (31) and (34) an initial condition  $\rho_0 = |a\rangle\langle a|$  was used. This is the proper equilibrium solution in the absence of fields for our choice of  $\gamma$  parameters. An equation system equivalent to eq. (34) was reported earlier by Bloembergen and Shen [21]. The perturbation matrices differ in the first row for the steady-state and the Laplace-transform problem. In the following applications we will solve eq. (31) for various combinations of “strong” and “weak” fields.

### 5.1. All fields treated as perturbations

If all fields are treated as perturbations, the zero-order matrix  $\mathbf{X}_0 - s\mathbf{1}$  contains only the three feeding parameters as non-diagonal elements. The corresponding  $3 \times 3$  block can easily be inverted:

$$\begin{bmatrix} -s & \gamma_{ba} & \gamma_{ca} \\ 0 & -\Gamma_{bb} - s & \gamma_{cb} \\ 0 & 0 & -\Gamma_{cc} - s \end{bmatrix}^{-1} = - \begin{bmatrix} \frac{1}{s} & \frac{\gamma_{ba}}{s(\Gamma_{bb} + s)} & \frac{\gamma_{ba}\gamma_{cb} + \gamma_{ca}(\Gamma_{bb} + s)}{s(\Gamma_{bb} + s)(\Gamma_{cc} + s)} \\ 0 & \frac{1}{\Gamma_{bb} + s} & \frac{\gamma_{cb}}{(\Gamma_{bb} + s)(\Gamma_{cc} + s)} \\ 0 & 0 & \frac{1}{\Gamma_{cc} + s} \end{bmatrix} \quad (35)$$

and the remaining matrix elements of the matrix  $(\mathbf{X}_0 - s\mathbf{1})^{-1}$  are the diagonal elements  $-(i\Delta_{ab} + s)^{-1}$ , etc. The zero-order solution according to eq. (30b) therefore is

$$r^{(0)} = [1/s, 0, 0, 0, 0, 0, 0, 0, 0] \quad (36)$$

and after performing the product  $(\mathbf{X}_0 - s\mathbf{1})^{-1} \cdot \mathbf{W}$ , eq. (30) takes the explicit form

$$\begin{bmatrix} r_{aa}^{(n)} \\ r_{bb}^{(n)} \\ r_{cc}^{(n)} \\ r_{ab}^{(n)} \\ r_{ba}^{(n)} \\ r_{ac}^{(n)} \\ r_{bc}^{(n)} \\ r_{ca}^{(n)} \\ r_{cb}^{(n)} \end{bmatrix} = \begin{bmatrix} 0 & 0 & 0 & \frac{-iW_1^*}{\Gamma_{bb}+s} & \frac{iW_1}{\Gamma_{bb}+s} & -ig_1W_2^* & ig_3W_3^* & ig_1W_2 & -ig_3W_3 \\ 0 & 0 & 0 & \frac{iW_1^*}{\Gamma_{bb}+s} & \frac{-iW_1}{\Gamma_{bb}+s} & ig_2W_2^* & -ig_4W_3^* & -ig_2W_2 & ig_4W_3 \\ 0 & 0 & 0 & 0 & 0 & \frac{iW_2^*}{\Gamma_{cc}+s} & \frac{iW_3^*}{\Gamma_{cc}+s} & \frac{-iW_2}{\Gamma_{cc}+s} & \frac{-iW_3}{\Gamma_{cc}+s} \\ \frac{-W_1}{\Delta_{ab}-is} & \frac{W_1}{\Delta_{ab}-is} & 0 & 0 & 0 & \frac{-W_3^*}{\Delta_{ab}-is} & 0 & 0 & \frac{W_2}{\Delta_{ab}-is} \\ \frac{-W_1^*}{\Delta_{ab}^*+is} & \frac{W_1^*}{\Delta_{ab}^*+is} & 0 & 0 & 0 & 0 & \frac{W_2^*}{\Delta_{ab}^*+is} & \frac{-W_3^*}{\Delta_{ab}^*+is} & 0 \\ \frac{-W_2}{\Delta_{ac}-is} & 0 & \frac{W_2}{\Delta_{ac}-is} & \frac{-W_3}{\Delta_{ac}-is} & 0 & 0 & \frac{W_1}{\Delta_{ac}-is} & 0 & 0 \\ 0 & \frac{-W_3}{\Delta_{bc}-is} & \frac{W_3}{\Delta_{bc}-is} & 0 & \frac{-W_2}{\Delta_{bc}-is} & \frac{W_1^*}{\Delta_{bc}-is} & 0 & 0 & 0 \\ \frac{-W_2^*}{\Delta_{ac}^*+is} & 0 & \frac{W_2^*}{\Delta_{ac}^*+is} & 0 & \frac{-W_3^*}{\Delta_{ac}^*+is} & 0 & 0 & 0 & \frac{W_1^*}{\Delta_{ac}^*+is} \\ 0 & \frac{-W_3^*}{\Delta_{bc}^*+is} & \frac{W_3^*}{\Delta_{bc}^*+is} & \frac{-W_2^*}{\Delta_{bc}^*+is} & 0 & 0 & 0 & \frac{W_1}{\Delta_{bc}^*+is} & 0 \end{bmatrix}^n \begin{bmatrix} 1/s \\ 0 \\ 0 \\ 0 \\ 0 \\ 0 \\ 0 \\ 0 \\ 0 \end{bmatrix}, \quad (37)$$

where

$$g_1 = \frac{\Gamma_{bb} + \gamma_{cb} + s}{(\Gamma_{bb} + s)(\Gamma_{cc} + s)}, \quad g_2 = \frac{\gamma_{cb}}{(\Gamma_{bb} + s)(\Gamma_{cc} + s)},$$

$$g_3 = \frac{\gamma_{ca} - \gamma_{ba}}{(\Gamma_{bb} + s)(\Gamma_{cc} + s)}, \quad g_4 = \frac{\gamma_{ca} + s}{(\Gamma_{bb} + s)(\Gamma_{cc} + s)}.$$

The only non-vanishing first-order results are, therefore

$$r_{ab}^{(1)} = r_{ba}^{(1)*} = -W_1/s(\Delta_{ab} - is), \quad (38a)$$

$$r_{ac}^{(1)} = r_{ca}^{(1)*} = -W_2/s(\Delta_{ac} - is), \quad (38b)$$

and the inverse Laplace transform yields

$$\tilde{\rho}_{ab}^{(1)}(t) = (W_1/\Delta_{ab})[\exp(-i\Delta_{ab}t) - 1], \quad (39a)$$

$$\tilde{\rho}_{ac}^{(1)}(t) = (W_2/\Delta_{ac})[\exp(-i\Delta_{ac}t) - 1], \quad (39b)$$

from which the steady-state values are obvious.

The second iteration of eq. (37) yields the population terms:



$$r_{aa}^{(2)} = -\frac{2(\Gamma_{ab} + s)}{s(\Gamma_{bb} + s)} \frac{W_1 W_1^*}{(\Delta_{ab} - is)(\Delta_{ab}^* + is)} - \frac{2(\Gamma_{ac} + s)(\gamma_{cb} + \gamma_{ba} + s)}{s(\Gamma_{bb} + s)(\Gamma_{cc} + s)} \frac{W_2 W_2^*}{(\Delta_{ac} - is)(\Delta_{ac}^* + is)}, \quad (40a)$$

$$r_{bb}^{(2)} = \frac{2(\Gamma_{ab} + s)}{s(\Gamma_{bb} + s)} \frac{W_1 W_1^*}{(\Delta_{ab} - is)(\Delta_{ab}^* + is)} + \frac{2(\Gamma_{ac} + s)\gamma_{cb}}{s(\Gamma_{bb} + s)(\Gamma_{cc} + s)} \frac{W_2 W_2^*}{(\Delta_{ac} - is)(\Delta_{ac}^* + is)}, \quad (40b)$$

$$r_{cc}^{(2)} = \frac{2(\Gamma_{ac} + s)}{s(\Gamma_{cc} + s)} \frac{W_2 W_2^*}{(\Delta_{ac} - is)(\Delta_{ac}^* + is)} \quad (40c)$$

and the coherent terms:

$$r_{ab}^{(2)} = r_{ba}^{(2)*} = \frac{W_2 W_3^*}{s(\Delta_{ab} - is)(\Delta_{ac} - is)}, \quad (41a)$$

$$r_{ac}^{(2)} = r_{ca}^{(2)*} = \frac{W_1 W_3}{s(\Delta_{ac} - is)(\Delta_{ab} - is)}, \quad (41b)$$

$$r_{bc}^{(2)} = r_{cb}^{(2)*} = \frac{W_2 W_1^*}{s(\Delta_{bc} - is)} \left[ \frac{1}{\Delta_{ab}^* + is} - \frac{1}{\Delta_{ac} - is} \right]. \quad (41c)$$

Since all the zeros of the denominators are obvious the Laplace back transform is straightforward but will not be reproduced here. In the general case the time development of the density matrix elements may become rather complicated, but for times longer than the relaxation parameters the steady-state solution may apply, which is easily found using eq. (22). In this limit eqs. (41a)–(41c) reduce to the second-order resonant susceptibilities already discussed in an earlier paper [22]. The feeding terms enter the formulas for the second-order populations (*dc* terms), but do not affect the coherence terms in second order.

In third order the population terms become proportional to the product of all three Rabi frequencies. Since we want to allow no more than two ingoing beams these terms vanish as long as the coupling with the generated wave is neglected. The third-order off-diagonal elements are

$$r_{ab}^{(3)} = \frac{4(\Gamma_{ab} + s)}{s(\Gamma_{bb} + s)} \frac{W_1^* W_1 W_1}{(\Delta_{ab}^* + is)(\Delta_{ab} - is)(\Delta_{ab} - is)} \quad (42a)$$

$$+ \frac{2(\Gamma_{ac} + s)(2\gamma_{cb} + \gamma_{ba} + s)}{s(\Gamma_{bb} + s)(\Gamma_{cc} + s)} \frac{W_1 W_2 W_2^*}{(\Delta_{ab} - is)(\Delta_{ac} - is)(\Delta_{ac}^* + is)} \quad (42b)$$

$$- \frac{W_1 W_3 W_3^*}{s(\Delta_{ab} - is)(\Delta_{ac} - is)(\Delta_{ab} - is)} \quad (42c)$$

$$+ \frac{W_1 W_2 W_2^*}{s(\Delta_{ab} - is)(\Delta_{bc}^* + is)} \left[ \frac{1}{\Delta_{ab} - is} - \frac{1}{\Delta_{ac}^* + is} \right], \quad (42d)$$

$$r_{bc}^{(3)} = -\frac{2(\Gamma_{ab} + s)}{s(\Gamma_{bb} + s)} \frac{W_1 W_1^* W_3}{(\Delta_{ab} - is)(\Delta_{ab}^* + is)(\Delta_{bc} - is)} \quad (42e)$$

$$+ \frac{2(\Gamma_{ac} + s)(\gamma_{ba} - \gamma_{cb} + s)}{s(\Gamma_{bb} + s)(\Gamma_{cc} + s)} \frac{W_2 W_2^* W_3}{(\Delta_{ac} - is)(\Delta_{ac}^* + is)(\Delta_{bc} - is)} \quad (42f)$$

$$- \frac{W_2 W_2^* W_3}{s(\Delta_{bc} - is)(\Delta_{ab}^* + is)(\Delta_{ac}^* + is)} \quad (42g)$$

$$+ \frac{W_1 W_1^* W_3}{s(\Delta_{bc} - is)(\Delta_{ac} - is)(\Delta_{ab} - is)}, \quad (42h)$$

$$r_{ac}^{(3)} = \frac{2(\Gamma_{ac} + s)(2\gamma_{ba} + \gamma_{cb} + 2s)}{s(\Gamma_{bb} + s)(\Gamma_{cc} + s)} \frac{W_2 W_2^* W_2}{(\Delta_{ac} - is)(\Delta_{ac} - is)(\Delta_{ac}^* + is)} \quad (42i)$$

$$+ \frac{2(\Gamma_{ac} + s)}{s(\Gamma_{cc} + s)} \frac{W_1 W_1^* W_2}{(\Delta_{ab} - is)(\Delta_{ab}^* + is)(\Delta_{ac} - is)} \quad (42k)$$

$$- \frac{W_2 W_3 W_3^*}{s(\Delta_{ac} - is)(\Delta_{ab} - is)(\Delta_{ac} - is)} \quad (42l)$$

$$+ \frac{W_1 W_1^* W_2}{s(\Delta_{ac} - is)(\Delta_{bc} - is)} \left[ \frac{1}{\Delta_{ab}^* + is} - \frac{1}{\Delta_{ac} - is} \right]. \quad (42m)$$

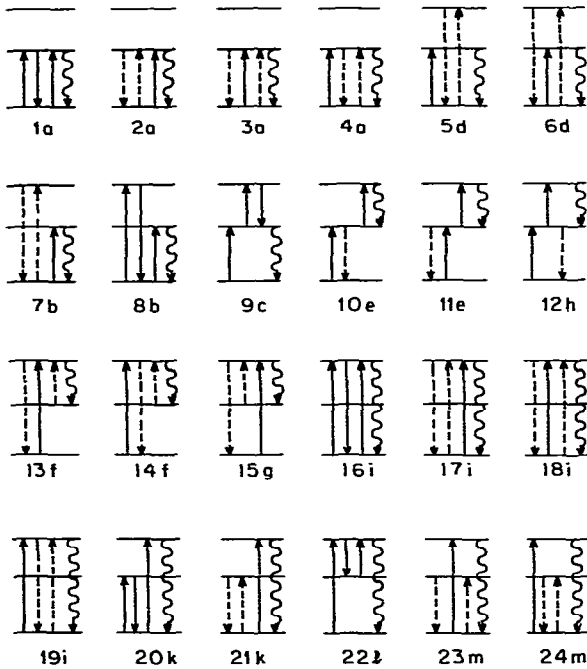


Fig. 2. Diagrammatic representation of the third-order contributions to the density operator in a fully resonant three-level system. Time ordering is from left to right. Full and broken lines describe evolution of the bra and ket part of the density operator, respectively. Direction of the arrows, upward or downward, refers to annihilation or creation of photons. The letters a–m under each diagram refer to the corresponding term in eq. (42).

The terms (42a), (42b), (42e), (42f), (42i) and (42k) evolve from the second-order population terms and include feeding. The only terms which show the extra DICE [11,12] resonance are (42d) and (42m) both unaffected by feeding contributions.

A method has therefore been presented which will generate all non-linear fully resonant susceptibilities in a three-level system to arbitrary orders. Extension of the scheme to the four-level system is discussed below. The calculation is even easier if directly performed on the steady-state solution. (That is, replace  $1/s$  by 1 and  $s$  by 0 in eq. (37).)

It should be noted, that *each* of the terms in (42a)–(42m) corresponds to *several* diagrams in the usual time-ordered iterative integration scheme. To illustrate this the conventional time-ordered diagrams that correspond to the terms (42a)–(42m) are collected in fig. 2. Eqs. (42) could be made more compact by extracting common multipliers and denominators. We have not done this in order to make more transparent which of the terms are singled out in an actual experiment. Thus, for example, an experiment with  $\omega_1$  and  $\omega_2$  as ingoing beams and observing the signal at  $\omega_1$  (which means  $r_{ab}$ ) is described by terms (42b) (population type) and (42d) (coherence type), and the corresponding conventional diagrams are numbered 5–8.

### 5.2. Solution for a strong $\omega_1$ field

The terms  $W_1$  and  $W_1^*$  are now retained in the zero-order  $\mathbf{X}^0$  matrix which then breaks up into three diagonal blocks indicated by the broken lines in eq. (31) and eq. (34), respectively. The zero-order solution for the two  $2 \times 2$  blocks has the trivial result

$$r_{ac}^{(0)} = r_{ca}^{(0)} = r_{bc}^{(0)} = r_{cb}^{(0)} = 0. \quad (43a)$$

The remaining  $5 \times 5$  linear equation system can be solved leading to

$$r_{aa}^{(0)} = [1/s D_1(s)] [(\Gamma_{bb} + s)(\Delta_{ab} - is)(\Delta_{ab}^* + is) + 2W_1 W_1^*(\Gamma_{ab} + s)], \quad (43b)$$

$$r_{bb}^{(0)} = [1/s D_1(s)] 2W_1 W_1^*(\Gamma_{ab} + s), \quad (43c)$$

$$r_{cc}^{(0)} = 0, \quad (43d)$$

$$r_{ab}^{(0)} = -[1/s D_1(s)] W_1 (\Gamma_{bb} + s)(\Delta_{ab}^* + is) = r_{ba}^{(0)*}, \quad (43e)$$

with

$$D_1(s) = (\Gamma_{bb} + s)(\Delta_{ab} - is)(\Delta_{ab}^* + is) + 4W_1 W_1^*(\Gamma_{ab} + s). \quad (44)$$

The couplings  $W_2$  and  $W_3$  can now be treated as perturbations, the vector  $\mathbf{Y} = -\mathbf{W} \cdot \mathbf{r}^{(0)}$  has only the following non-zero elements:

$$Y_{ac} = Y_{ca}^* = iW_2 r_{aa}^{(0)} + iW_3 r_{ab}^{(0)}, \quad (45a)$$

$$Y_{bc} = Y_{cb}^* = iW_3 r_{bb}^{(0)} + iW_2 r_{ba}^{(0)}. \quad (45b)$$

Eq. (29) for the first-order results reduces therefore to two  $2 \times 2$  problems which are complex conjugates. The solution is

$$\begin{pmatrix} r_{ac}^{(1)} \\ r_{bc}^{(1)} \end{pmatrix} = \frac{i}{F_1(s)} \begin{pmatrix} \Delta_{bc} - is & W_1 \\ W_1^* & \Delta_{ac} - is \end{pmatrix} \begin{pmatrix} Y_{ac} \\ Y_{bc} \end{pmatrix}, \quad (46)$$

where  $F_1(s) = (\Delta_{ac} - is)(\Delta_{bc} - is) - W_1 W_1^*$ , leading to the final result

$$r_{ac}^{(1)} = -[W_2/sD_1(s)F_1(s)] \{(\Gamma_{bb} + s)(\Delta_{ab} - is)(\Delta_{ab}^* + is)(\Delta_{bc} - is) + W_1 W_1^* [2(\Gamma_{ab} + s)(\Delta_{bc} - is) - (\Gamma_{bb} + s)(\Delta_{ab} - is)]\} \quad (47a)$$

$$+ [W_1 W_3/sD_1(s)F_1(s)] [(\Gamma_{bb} + s)(\Delta_{bc} - is)(\Delta_{ab}^* + is) - 2W_1 W_1^*(\Gamma_{ab} + s)] , \quad (47b)$$

$$r_{bc}^{(1)} = -[W_1^* W_2/sD_1(s)F_1(s)] [(\Gamma_{bb} + s)(\Delta_{ab} - is)(\Delta_{ab}^* - \Delta_{ac} + 2is) + 2W_1 W_1^*(\Gamma_{ab} + s)] \quad (47c)$$

$$- [W_1 W_1^* W_3/sD_1(s)F_1(s)] [2(\Gamma_{ab} + s)(\Delta_{ac} - is) - (\Gamma_{bb} + s)(\Delta_{ab}^* + is)] . \quad (47d)$$

The resulting terms have been grouped in such a way, that each of the four formulas (47a)–(47d) corresponds to a certain choice of ingoing and observed waves. In a particular experiment one will therefore have only to deal with the appropriate term.

The relation between each term and its corresponding experiment is symbolized in fig. 3, where we also included a diagram corresponding to the “zero-order” equation (43e). In contrast to fig. 2 the arrows no longer indicate development of the bra or ket term and no time ordering is intended to be shown. In fact, eq. (47c) contains both time orderings of  $\omega_1$  and  $\omega_2$  which can easily be verified by expanding (47c) in powers of  $W_1$  and comparing the result with (41c). In a similar way, expansion of (47a) leads to the first-order term (38b) and the third-order terms (42k) and (42m), the latter containing the diagrams numbered 23 and 24 of fig. 2 leading to the DICE resonances, previously discussed by us in relation to difference-frequency generation [22].

### 5.3. Solution for a strong $\omega_2$ field

The treatment of a strong  $\omega_2$  field is completely analogous to the previous case in section 4.2. Again the  $\mathbf{X}^0$  matrix can be blocked by arranging the rows and columns in the order  $aa, bb, cc, ac, ca, ab, cb, ba, bc$  to yield a  $5 \times 5$  and two  $2 \times 2$  problems. Due to the feeding from level  $c$  to  $b$ , however, all three populations are now differ-

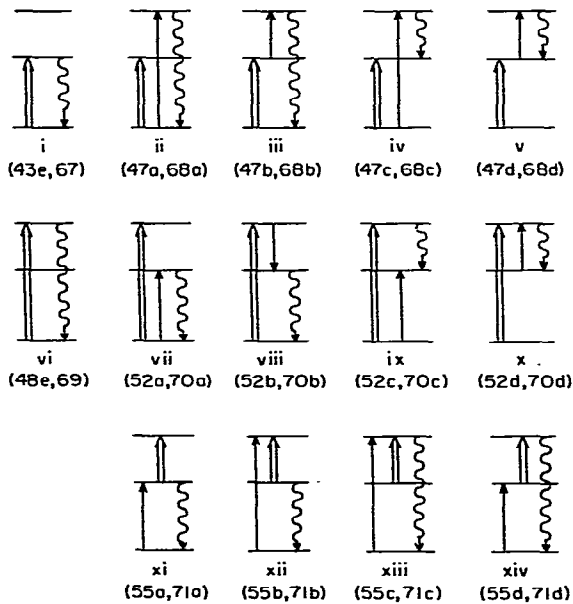


Fig. 3. Schematic representation of the various terms resulting from the calculation of a fully resonant three-level system under the influence of one strong field (thick arrow) and one weak field (thin arrow). The generated wave is indicated by the wavy arrow. Below each diagram corresponding to an experimental configuration the appropriate formula numbers for the Laplace-transform result and the steady-state result are given. Contrary to those in fig. 2 the diagrams cannot be interpreted as representing a certain time ordering.

ent from zero. The zero-order solutions are

$$r_{ab}^{(0)} = r_{cb}^{(0)} = r_{ba}^{(0)} = r_{bc}^{(0)} = 0 \quad (48a)$$

and

$$r_{aa}^{(0)} = [(\Gamma_{bb} + s)/sD_2(s)] [(\Delta_{ac}^* + is)(\Delta_{ac} - is)(\Gamma_{cc} + s) + 2W_2W_2^*(\Gamma_{ac} + s)] , \quad (48b)$$

$$r_{bb}^{(0)} = [1/sD_2(s)] 2W_2W_2^*\gamma_{cb}(\Gamma_{ac} + s) , \quad (48c)$$

$$r_{cc}^{(0)} = [1/sD_2(s)] 2W_2W_2^*(\Gamma_{ac} + s)(\Gamma_{bb} + s) , \quad (48d)$$

$$r_{ac}^{(0)} = -[W_2/sD_2(s)](\Delta_{ac}^* + is)(\Gamma_{cc} + s)(\Gamma_{bb} + s) = r_{ca}^{(0)*} , \quad (48e)$$

with

$$D_2(s) = (\Delta_{ac} - is)(\Delta_{ac}^* + is)(\Gamma_{cc} + s)(\Gamma_{bb} + s) + 2W_2W_2^*(\Gamma_{ac} + s)(2\Gamma_{bb} + \gamma_{cb} + 2s) . \quad (49)$$

Now the perturbations were  $W_1$  and  $W_3$ , and the non-zero elements of the vector  $Y = -W \cdot r^{(0)}$  are

$$Y_{ab} = iW_1(r_{aa}^{(0)} - r_{bb}^{(0)}) + iW_3^*r_{ac}^{(0)} , \quad (50a)$$

$$Y_{cb} = iW_3^*(r_{cc}^{(0)} - r_{bb}^{(0)}) + iW_1r_{ca}^{(0)} . \quad (50b)$$

The first-order problem reduces again to a single  $2 \times 2$  problem:

$$\begin{pmatrix} r_{ab}^{(1)} \\ r_{cb}^{(1)} \end{pmatrix} = \frac{i}{F_2(s)} \begin{pmatrix} \Delta_{bc}^* + is & -W_2 \\ -W_2^* & -\Delta_{ab} + is \end{pmatrix} \begin{pmatrix} Y_{ab} \\ Y_{cb} \end{pmatrix} , \quad (51)$$

which yields

$$r_{ab}^{(1)} = [W_1/sD_2(s)F_2(s)] \{ [2(\Gamma_{ac} + s)(\gamma_{cb} - \Gamma_{bb} - s)(\Delta_{bc}^* + is) - (\Delta_{ac} - is)(\Gamma_{cc} + s)(\Gamma_{bb} + s)] W_2W_2^* - (\Delta_{ac}^* + is)(\Delta_{ac} - is)(\Gamma_{cc} + s)(\Gamma_{bb} + s)(\Delta_{bc}^* + is) \} \quad (52a)$$

$$+ [W_2W_3^*/sD_2(s)F_2(s)] [(\Delta_{bc}^* + is)(\Delta_{ac}^* + is)(\Gamma_{cc} + s)(\Gamma_{bb} + s) - 2W_2W_2^*(\Gamma_{ac} + s)(\gamma_{cb} - \Gamma_{bb} - s)] . \quad (52b)$$

$$r_{cb}^{(1)} = [W_1W_2^*/sD_2(s)F_2(s)] [(\Gamma_{cc} + s)(\Gamma_{bb} + s)(\Delta_{ac} - is)(\Delta_{ac}^* - \Delta_{ab} + 2is) + 2W_2W_2^*(\Gamma_{ac} + s)(\Gamma_{bb} - \gamma_{cb} + s)] \quad (52c)$$

$$+ [W_2W_2^*W_3^*/sD_2(s)F_2(s)] [2(\Delta_{ab} - is)(\Gamma_{ac} + s)(\Gamma_{bb} - \gamma_{cb} + s) - (\Delta_{ac}^* + is)(\Gamma_{cc} + s)(\Gamma_{bb} + s)] , \quad (52d)$$

where  $F_2(s) = (\Delta_{ab} - is)(\Delta_{bc}^* + is) + W_2^*W_2$ . Again each term corresponds to a certain choice of experimental conditions as indicated in the diagrams vi–x in fig. 3.

#### 5.4. Solution for a strong $\omega_3$ field

For this case blocking of the  $X^0$  matrix is achieved by the index ordering  $aa, bb, cc, bc, cb, ab, ac, ba, ca$ . Solution of the zero-order problem yields as the only non-vanishing element:

$$r_{aa}^{(0)} = 1/s, \quad (53)$$

corresponding to  $\tilde{\rho}_{aa} = 1$ . The strong  $\omega_3$  field alone has, therefore, no effect since both levels  $b$  and  $c$  have no equilibrium population. The first-order problem thus takes the simple form

$$\begin{pmatrix} \Delta_{ab} - is & W_3^* \\ W_3 & \Delta_{ac} - is \end{pmatrix} \begin{pmatrix} r_{ab}^{(1)} \\ r_{ac}^{(1)} \end{pmatrix} = - \begin{pmatrix} W_1/s \\ W_2/s \end{pmatrix} \quad (54)$$

and the solution reads

$$r_{ab}^{(1)} = -W_1(\Delta_{ac} - is)/sF_3(s) + W_2W_3^*/sF_3(s), \quad (55a,b)$$

$$r_{ac}^{(1)} = -W_2(\Delta_{ab} - is)/sF_3(s) + W_1W_3/sF_3(s), \quad (55c,d)$$

with

$$F_3(s) = (\Delta_{ab} - is)(\Delta_{ac} - is) - W_3W_3^*. \quad (55e)$$

The corresponding diagrams are shown as xi–xiv in fig. 3.

### 5.5. Convergence of perturbation approach

On the basis of these results we may now specify more precisely what is a “strong” and a “weak” field in this approach. We have already seen that expansion of the strong-field results in powers of the strong field may yield the results of the conventional perturbation theory expansion of the density operator as found in eqs. (38)–(42). If such an expansion were to converge sufficiently rapidly, the field treated as “strong” would be sufficiently weak for perturbation theory to be valid. From eq. (43e) we can deduce the following convergence condition:

$$4W_1W_1^*(\Gamma_{ab} + s)/(\Gamma_{bb} + s)(\Delta_{ab} - is)(\Delta_{ab}^* + is) < 1, \quad (56)$$

which on resonance reduces to

$$4W_1W_1^*/\Gamma_{bb}\Gamma_{ab} < 1. \quad (57)$$

From eq. (46) we obtain a similar condition, namely

$$W_1W_1^*/\Gamma_{ac}\Gamma_{bc} < 1. \quad (58)$$

Similar relations are found for  $W_2$  and  $W_3$  from eqs. (48), (51) and (55).

## 6. Transient effects

To study transient phenomena we require the Laplace back transforms for the formulas derived in the previous section. This is usually done by first expanding the Laplace-transformed formula in partial fractions:

$$r(s) = \sum_{i=1}^n \frac{c_i}{s - s_i}, \quad (59)$$

where  $s_i$  are the first-order poles of  $r(s)$  that are considered here and the coefficients  $c_i$  are found through

$$c_i = \lim_{s \rightarrow s_i} (s - s_i)r(s). \quad (60)$$

The back transform in the time domain then is

$$\tilde{\rho}(t) = \sum_{i=1}^n c_i \exp(s_i t). \quad (61)$$

The real part of a pole  $s_i$ , therefore, describes the damping of the signal. All formulas of the preceding section contain the pole  $s_0 = 0$  corresponding to the time-independent – steady-state – solution. The function  $r(s)$  has the form:  $r(s) = f(s)/g(s)$ , so that the poles are found as the zeros of  $g(s) = \prod_i (s - s_i)$ , and eq. (60) has the solution

$$c_i = f(s_i) \left[ \prod_{k \neq i} (s_k - s_i) \right]^{-1}, \quad (62)$$

which is readily adopted to numerical procedures. The zeros of  $g(s)$  may be found numerically, but under fully resonant conditions the results are sufficiently simple to obtain that a numerical analysis is unnecessary. These analytic results are discussed below.

All terms connected with the strong  $\omega_1$  field contain the factor  $D_1(s)$  [see eq. (44)] in the denominator, which in the case of full resonance has zeros at  $s_1 = -\Gamma_{ab}$ , and  $s_{2,3} = -\frac{1}{2}(\Gamma_{ab} + \Gamma_{bb} \pm i\Omega_a)$ . Thus if the  $\omega_1$  field is strong enough such that  $\Omega_a = [16|W_1|^2 - (\Gamma_{bb} - \Gamma_{ab})^2]^{1/2}$  is real, the signal is expected to decay with a time constant  $\Gamma_{bb} + \Gamma_{ab}$  and nutate with frequency  $\Omega_a$ . The perturbation with the  $W_2$  and  $W_3$  fields involves the factor  $F_1(s)$  which has zeros at

$$s_{4,5} = -\frac{1}{2}i\{\Delta_{ac} + \Delta_{bc} \pm [(\Delta_{ac} - \Delta_{bc})^2 + 4W_1W_1^*]^{1/2}\}. \quad (63)$$

In the case of full resonance this reduces to

$$s_{4,5} = -\frac{1}{2}i\{\Gamma_{ac} + \Gamma_{bc} \pm i[4W_1W_1^* - (\Gamma_{ac} - \Gamma_{bc})^2]^{1/2}\}. \quad (64)$$

So if the  $W_1$  field is large enough to make the expression under the square root positive, oscillation will occur with frequency

$$\Omega_b = [4W_1W_1^* - (\Gamma_{ac} - \Gamma_{bc})^2]^{1/2}. \quad (65)$$

Thus a strong  $\omega_1$  field will cause the non-linear signal at  $\omega_2$  or  $\omega_3$  in the experiments shown in diagrams ii–v of fig. 3 to ring with two frequencies having the ratio  $\Omega_a : \Omega_b = 2 : 1$ . Of special interest, however, is the intensity range in which the oscillations begin to evolve, since such experiments should yield information about the corresponding relaxation parameters. Our results show that the decay rate is the sum of two  $\Gamma$  parameters, but that the onset of oscillation is determined by their difference. Therefore, both  $\Gamma$  parameters might be extracted from measurements of this transient behavior.

In the case of a strong  $\omega_2$  field the situation is somewhat more complicated as a result of the presence of the feeding term  $\gamma_{cb}$ , which causes  $D_2(s)$  to be of fourth order in  $s$ . If we choose  $\gamma_{cb} = 0$  explicit results are found to be as given in eqs. (63)–(65) after replacing  $(W_1, \Gamma_{ab}, \Gamma_{bb}, \Gamma_{ac}, \Gamma_{bc})$  by  $(W_2, \Gamma_{ac}, \Gamma_{cc}, \Gamma_{ab}, \Gamma_{bc})$ . The case  $\gamma_{cb} \neq 0$  is best solved numerically. Finally, in the case that  $\omega_3$  is the only strong field, only two non-zero roots exist of the type of eq. (63)

$$s_{1,2} = -\frac{1}{2}i\{\Delta_{ab} + \Delta_{ac} \pm [(\Delta_{ab} - \Delta_{ac})^2 + 4W_3W_3^*]^{1/2}\}. \quad (66)$$

with the on-resonance solution given according to eqs. (64) and (65).

## 7. Lineshapes

Of great interest in non-linear spectroscopy are the influences of field intensity on the steady-state response. For the strong field being  $\omega_1$  we find:

$$\tilde{\rho}_{ab} = -\Gamma_{bb} \Delta_{ab}^* W_1 / D_1(0) , \quad (67)$$

$$\tilde{\rho}_{ac} = [W_2 / D_1(0) F_1(0)] [W_1 W_1^* (\Gamma_{bb} \Delta_{ab} - 2\Gamma_{ab} \Delta_{bc}) - \Gamma_{bb} \Delta_{ab} \Delta_{ab}^* \Delta_{bc}] \quad (68a)$$

$$+ [W_1 W_3 / D_1(0) F_1(0)] (\Gamma_{bb} \Delta_{bc} \Delta_{ab}^* - 2\Gamma_{ab} W_1 W_1^*) , \quad (68b)$$

$$\tilde{\rho}_{bc} = [W_2 W_1^* / D_1(0) F_1(0)] [\Gamma_{bb} \Delta_{ab} (\Delta_{ac} - \Delta_{ab}^*) - 2\Gamma_{ab} W_1 W_1^*] \quad (68c)$$

$$+ [W_1 W_1^* W_3 / D_1(0) F_1(0)] (\Gamma_{bb} \Delta_{ab}^* - 2\Gamma_{ab} \Delta_{ac}) . \quad (68d)$$

The results for a strong  $\omega_2$  field are

$$\tilde{\rho}_{ac} = -W_2 \Gamma_{bb} \Gamma_{cc} \Delta_{ac}^* / D_2(0) , \quad (69)$$

$$\tilde{\rho}_{ab} = [W_1 / D_2(0) F_2(0)] \{ W_2 W_2^* [2\Gamma_{ac} \Delta_{bc}^* (\gamma_{cb} - \Gamma_{bb}) - \Gamma_{bb} \Gamma_{cc} \Delta_{ac}] - \Delta_{ac} \Delta_{ac}^* \Delta_{bc}^* \Gamma_{bb} \Gamma_{cc} \} \quad (70a)$$

$$+ [W_3 W_2 / D_2(0) F_2(0)] [\Delta_{bc}^* \Delta_{ac}^* \Gamma_{cc} \Gamma_{bb} + 2W_2 W_2^* \Gamma_{ac} (\Gamma_{bb} - \gamma_{cb})] , \quad (70b)$$

$$\tilde{\rho}_{cb} = [W_1 W_2^* / D_2(0) F_2(0)] [\Gamma_{bb} \Gamma_{cc} \Delta_{ac} (\Delta_{ac}^* - \Delta_{ab}) + 2W_2 W_2^* \Gamma_{ac} (\Gamma_{bb} - \gamma_{cb})] \quad (70c)$$

$$+ [W_2 W_2^* W_3 / D_2(0) F_2(0)] [2\Gamma_{ac} \Delta_{ab} (\Gamma_{bb} - \gamma_{cb}) - \Gamma_{cc} \Gamma_{bb} \Delta_{ac}^*] . \quad (70d)$$

Finally for the case that the  $\omega_3$  field is strong we obtain

$$\tilde{\rho}_{ab} = -W_1 \Delta_{ac} / F_3(0) + W_2 W_3^* / F_3(0) , \quad (71a,b)$$

$$\tilde{\rho}_{ac} = -W_2 \Delta_{ab} / F_3(0) + W_1 W_3 / F_3(0) . \quad (71c,d)$$

The corresponding diagrams in fig. 3 are labelled with the appropriate formula number in order to make the identification of the experimental conditions involved more obvious.

In the thin-sample approximation (neglect of depletion of the pump fields) it follows from Maxwell's equation that the intensity of each generated wave at  $\omega_1$ ,  $\omega_2$  or  $\omega_3$  is proportional to the square of the corresponding density matrix element, e.g.

$$I(\omega_1) \propto |\mu_{ab} \tilde{\rho}_{ba}|^2 = |\mu_{ab}|^2 |\tilde{\rho}_{ab}|^2 . \quad (72)$$

Since these expressions contain resonance terms,  $\Delta_{\mu\nu}$ , both in the denominators and numerators the lineshapes are in general complicated and non-lorentzian. For some cases we will give an analytic discussion, for others we will show the results of numerical simulations. Two important experimental conditions may be distinguished: one in which the strong field is tuned, and the other, in which the perturbation field is scanned.

In the simplest experiment the strong field is scanned and the signal observed at the same frequency, with no additional fields present. The corresponding diagram is fig. 3i, and eq. (67) [or, equivalently, fig. 3vi with eq. (69)]. With the definition of detuning  $\delta = \omega_{ba} - \omega_1$  the square of eq. (67) has extrema for

$$\delta_1 = 0 , \quad \delta_{2,3} = \pm(x^2 - 1)^{1/2} \Gamma_{ab} , \quad (73)$$

with

$$x^2 = 4W_1 W_1^* / \Gamma_{ab} \Gamma_{bb} . \quad (74)$$

For  $x < 1$  the intensity of the generated beam is predicted to have a maximum at  $\delta_1 = 0$ , while for  $x > 1$  this maximum splits into two maxima at  $\delta_2$  and  $\delta_3$  with  $\delta_1$  now being a minimum. The corresponding intensities are



$$I_1 = x^2 \Gamma_{ab} \Gamma_{bb} / 4(1 + x^2), \quad I_{2,3} = \Gamma_{bb} / 16 \Gamma_{ab}. \quad (75)$$

For large  $x$  the points of half intensity are at  $\delta = \pm(3 + 8^{1/2})^{1/2} \Gamma_{ab} x$ . Therefore the width of each peak and the peak separation will be  $2\Gamma_{ab} x$ . The result is that the width of the spectrum increases with increasing field strength. This well-known property of a two-level system is demonstrated in fig. 4 for several sets of parameters. Note that the upper level lifetime  $\Gamma_{bb} = \gamma_{ba}$  has a strong effect on the intensity parameter  $x$  and consequently on the lineshape.

The situation becomes more complicated in the presence of an additional weak field. The generated field may now have the same frequency as the weak field, or be the difference or sum frequency. The intensity effect can no longer be contracted to a single intensity parameter  $x$  like in the previous example. This means,  $W$ ,  $\gamma$  and  $\Gamma$  now act differently on the lineshape. As an example we consider the type II difference-frequency generation process of eq. (68c). Fig. 5 shows some simulated lineshapes corresponding to this process measured as a function of the strong frequency detuning. It is seen that increasing the value of  $W$  first broadens the line, then splits it into two lines which further broaden while they shift apart. Decreasing the value of  $\gamma_{ba}$ , however, leads to different behavior with the splitting into two peaks occurring in a different range or vanishing altogether at the stated field intensities when  $\gamma_{ba}$  becomes very small.

All experiments performed with the strong field scanned have in common that the observed linewidths are strongly affected by the Rabi frequency of the strong field so that the interesting molecular and relaxation parameters are not clearly exposed in such a scan.

We now consider the predictions for lineshapes obtained by scanning the weak field. One example concerns the difference-frequency generation type II process, eq. (68c). With the strong field  $\omega_1$  fixed to resonance, the condition  $\delta I / \delta \delta = 0$  leads to a polynomial of order 5 in  $\delta$ , which is defined as the detuning  $\delta = \omega_{ac} + \omega_2$ . One root of this polynomial is  $\delta_1 = 0$ , and two roots are always complex. Therefore only two situations are possible:

- (a) only one maximum at  $\delta_1 = 0$ ,
- (b) two maxima at  $\delta = \pm \delta_2 \approx W_1$  and a minimum at  $\delta = 0$ .

At sufficiently large field strengths  $W_1$  the line splits into two lines with separation  $2W_1$ . The widths of the two lines, however, are not affected by the field intensity. Varying the  $\Gamma_{\mu\nu}$  parameters in the model reveals that the

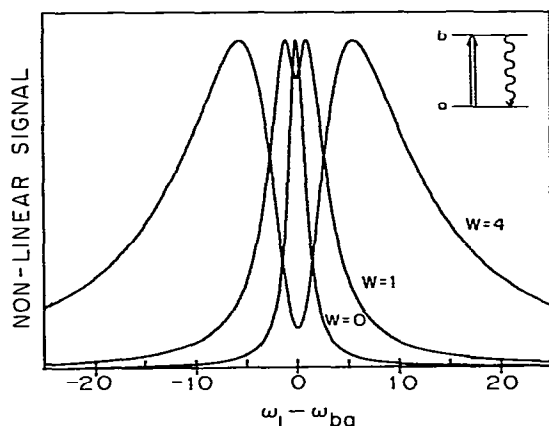


Fig. 4. Strong field response  $|\rho_{ab}|^2$  of a two-level system as a function of detuning from resonance. The parameter is the on-resonance Rabi frequency of the field.

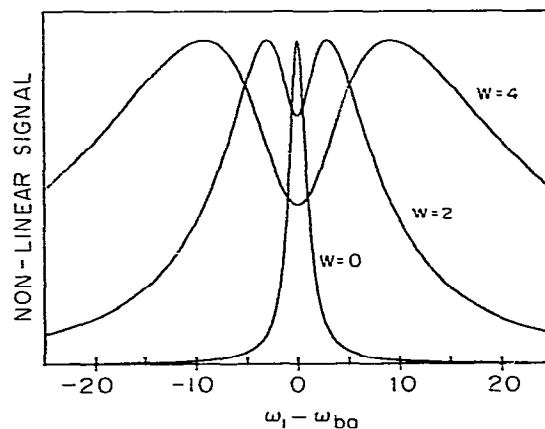


Fig. 5. Difference-frequency generation (type II) in a three-level system with one strong and one weak ingoing field. The weak field is fixed on resonance and the strong field scanned. The parameter is the strong-field Rabi frequency ( $\Gamma_{ab} = 1$ ,  $\Gamma_{bb} = 2$  fixed).

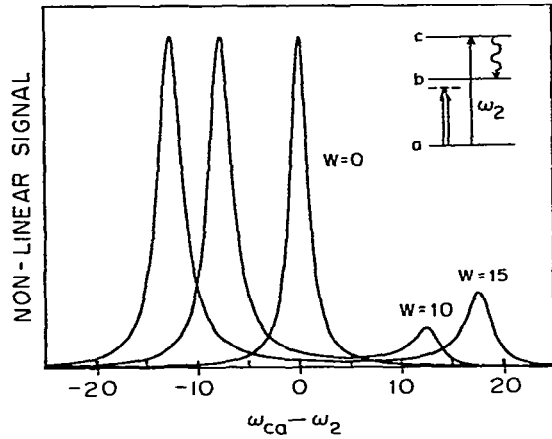


Fig. 6. Simulation of a pure power-induced extra resonance in type II difference-frequency generation. Parameters are: detuning  $\omega_{ba} - \omega_1 = 5$ ,  $\Gamma_{ac} = \Gamma_{ab} = 1$ ,  $\Gamma_{bc} = 2$ ,  $\gamma_{ba} = 2$ , corresponding to pure radiative damping.

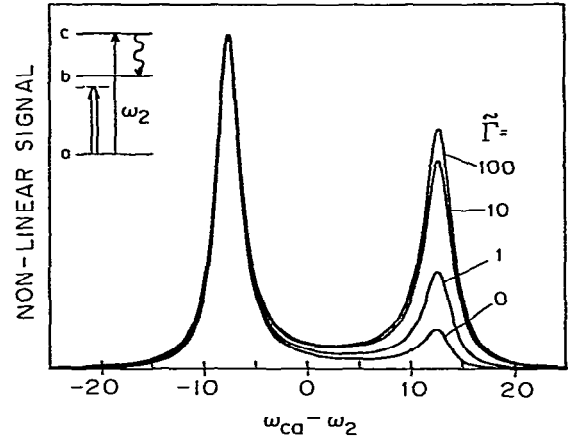


Fig. 7. Power effect on a DICE resonance. Parameters are  $\omega_{ba} - \omega_1 = 5$ ,  $\Gamma_{ac} = 1$ ,  $\Gamma_{bc} = 2$ ,  $W = 10$ ,  $\gamma_{ba} = 2$  in this simulation. The pure dephasing parameter  $\tilde{\Gamma}$  is changed from 0 to 100 by varying  $\Gamma_{ab}$ .

linewidth is essentially determined by the width of the resonance over which the weak field is tuned. If the strong field is detuned from resonance basically the same behavior is observed, but the two lines now have different intensity. This is simulated in fig. 6 for various strengths of the strong field. Detuning of the fixed frequency is the condition under which extra resonances of the DICE and PIER-4 type can be observed. Under these conditions the strong field creates two lines that are separated initially by the fixed frequency detuning. Both resonances shift with increasing field strength. The weaker resonance appears at the energy where the extra resonance is expected. Therefore, fig. 6 describes a pure power-induced extra resonance since the pure dephasing is set to zero. A further very interesting fact is that the lineshapes are found to be insensitive to the choice of the population decay parameter  $\gamma_{ba}$ . This is in contrast to what was found in the simulated spectra with the strong field scanned. In the purely perturbative treatment of the type II difference-frequency generation feeding parameters do not appear.

In fig. 7 the extra resonance is studied under conditions where both a strong field and pure dephasing are present. For a fixed value of  $W$  the pure dephasing parameter  $\tilde{\Gamma}$  is reduced from 100  $\Gamma_{ac}$  to 0. Obviously the general appearance of the signal is not changed. The difference in peak height in the limit  $\tilde{\Gamma} = 0$  is attributed to the detuning of the fixed frequency. Varying the parameters  $\Gamma_{bc}$  and  $\Gamma_{ac}$  it is found that both linewidths depend on both parameters. In the weak-field limit the DICE resonance has width  $\Gamma_{bc}$  while the other resonance has width  $\Gamma_{ac}$ . The strong field, therefore, not only can induce the extra resonance, but also affects its position and linewidths. The latter effect is, however, not power broadening but corresponds to a mixing of the character of the "normal" and the "extra" resonance which become undistinguishable at very high field strengths ( $W \gg \Gamma_{\mu\nu}$  and detuning). These results suggest that the DICE resonance observed in solids [11,12] and PIER-4 "extra" resonances seen in sodium vapor [19] might also be induced by sufficiently intense fields even in the absence of pure dephasing (solids) or collisional redistribution (gases). In section 7 it will be shown that this is indeed the situation for a four-level system.

## 8. Strong-field CARS and CSRS processes in a four-level system

The technique described here is not sufficiently general to handle Stokes and anti-Stokes Raman processes for all level schemes. However it does apply to CARS and CSRS in a four-level system which is a configuration readily

accessible to experiments. The two- and three-level responses in strong field can be calculated by another approach which involves a stepwise application of the rotating-wave approximation. These results will be discussed in a later publication.

CARS and CSRS processes in a four-level scheme are included in fig. 1. CARS involves effects resulting from  $W_2$ ,  $W_3$  and  $W_5$ , and explicit formulas can be obtained when  $W_2$  is considered to be a strong field. In most molecular systems if  $\omega_2$  is on-resonance with an electronic transition  $a \rightarrow c$  then it will be off-resonance for process  $b \rightarrow d$ . This implies that  $W_5$  can be considered as a weak-field effect for the case  $W_5 = \mu_{bc} \epsilon_2 \ll \hbar(\omega_{db} - \omega_2)$ . In a common situation this detuning would correspond to the difference in the vibrational frequencies ( $\omega_{ba}$  and  $\omega_{dc}$ ) of the ground and electronically excited states. Thus for many cases of interest  $W_5/c$  can be as large as  $5-50 \text{ cm}^{-1}$  and still be treated as a perturbation in the four-level problem. Similar considerations apply to the Stokes process using  $W_2$ ,  $W_4$  and  $W_5$  in the  $abcd$  four-level system of fig. 1b. The strong-field effect can be chosen as  $W_2$  and as before  $W_5$  can be chosen as a weak field for many cases of interest. The  $16 \times 16$  matrix  $\mathbf{X}$  for these four-level problems is given explicitly here (table 1) in terms of the possible six resonant Rabi parameters  $W_1$  to  $W_6$  and the six feeding terms  $\gamma_{ij}$ . These parameters along with the  $\Gamma$  completely define the four-level problem assuming that the temperature  $T$  is sufficiently low that  $kT$  is very much less than any of the energy separations. Results for any of the fields chosen as strong can be obtained numerically by inversion of the  $16 \times 16$  matrix.

The result for the CARS signal at  $2\omega_1 - \omega_2$  is obtained from the element  $\rho_{ad}^{(2)}$  which is found to be given as follows, with the definitions  $G_2(0) = \Delta_{ad} \Delta_{cd} - |W_2|^2$ ,  $g = \Gamma_{ac}(\Gamma_{bb} - \gamma_{cb})/\Gamma_{bb}\Gamma_{cc}$ :

$$\begin{aligned} \tilde{\rho}_{ad}^{(2)} = & -[W_2 W_3^* W_5 \Gamma_{bb} \Gamma_{cc} / G_2(0) F_2(0) D_2(0)] [\Delta_{cd} \Delta_{bc}^* \Delta_{ac} - W_2 W_2^* \Delta_{ac}^* + 2g W_2 W_2^* (\Delta_{cd} + \Delta_{ab})] \\ & - 2W_2^* W_2^2 W_3^* W_5 \Gamma_{bb} \Gamma_{cc} / D_2(0) G_2(0) \Delta_{bd} . \end{aligned} \quad (76)$$

This expression is exact in the case  $W_3$  and  $W_5$  represent weak-field effects, while  $W_2$  may have any value. When all fields are chosen as weak this expression reduces to the conventional CARS fully resonant expression that composes  $\chi^{(3)}$ , and terms that would conventionally be calculated from  $\chi^{(n)}$  with  $n \geq 5$ , odd. The conventional  $\chi^{(3)}$  term is

$$\chi_{\text{CARS}}^{(3)} = -\mu_{ac} \mu_{bc}^* \mu_{bd} \mu_{da} / \Delta_{ac} \Delta_{ad} \Delta_{ab} . \quad (77)$$

One interesting  $\chi^{(5)}$  term that depends on the existence of feeding is

$$\chi_{\text{CARS}}^{(5)} = -(2\Gamma_{ac} \gamma_{cb} / \Gamma_{cc} \Gamma_{bb}) \mu_{ac}^2 \mu_{ac}^* \mu_{bc}^* \mu_{bd} \mu_{da} / \Delta_{ac} \Delta_{ac}^* \Delta_{bd} \Delta_{ad} \Delta_{cd} . \quad (78)$$

The feeding term  $\chi_{\text{CARS}}^{(5)}$  contains an excited-state resonant term  $\Delta_{cd}$  normally only seen through the DICE or extra-resonance effect. Presumably eq. (76) is the proper expression to employ for studies of resonant CARS processes when  $\omega_1$  is an intense laser field near resonance to the transition  $a \rightarrow c$ . This result predicts resonances at both  $\omega_2 - \omega_3 = \omega_{ba}$  and  $\omega_2 - \omega_3 = \omega_{dc}$ , the  $\omega_{dc}$  resonance depends on  $\gamma_{bc}$  in the limit of weak fields.

Some CARS lineshapes are simulated in fig. 8 with  $\omega_2$  fixed on the  $a \rightarrow c$  resonance and  $\omega_3$  scanned. If both fields are weak two resonances appear at  $\omega_{ba} = \omega_2 - \omega_3$  and  $\omega_{da} = 2\omega_2 - \omega_3$ . With increasing strength of the  $\omega_2$  field each of the resonances splits symmetrically into two lines.

The corresponding Stokes signal at  $2\omega_2 - \omega_4$  ( $\omega_2 < \omega_4$ ) is obtained from the  $cb$  matrix element:

$$\begin{aligned} \tilde{\rho}_{cb}^{(2)} = & -[W_2^* W_4 W_5^* \Gamma_{bb} \Gamma_{cc} / D_2(0) F_2(0) G_2(0)] \{ \Delta_{cd} \Delta_{ac} \Delta_{ac}^* + \Delta_{ab} \Delta_{ac} (\Delta_{ac}^* - \Delta_{ad}) \\ & + W_2 W_2^* [(2\Gamma_{ac} / \Gamma_{cc}) (\Delta_{cd} + \Delta_{ab}) - \Delta_{ac}] \} + 2W_2^* W_2^2 W_4 W_5^* \Gamma_{ac} \gamma_{cb} / F_2(0) D_2(0) \Delta_{bd}^* . \end{aligned} \quad (79)$$

As with the CARS case the last term in (79) in the limit of all fields weak corresponds to a  $\chi^{(5)}$  process. This describes Stokes generation from the population created as a result of feeding from level  $c$  into level  $b$  through  $\gamma_{cb}$ .

Table 1

Explicit form of the matrix equation  $(\mathbf{X} - s\mathbf{I}) \cdot \mathbf{r} = -\boldsymbol{\rho}_0$  for a four-level system. The broken lines indicate the block diagonal form of the  $\mathbf{X}^0$  matrix if  $W_2$  is considered the only strong field to be present, as used for the discussion of CARS and CSRS in this paper

$-s$	$\gamma_{ba}$	$\gamma_{ca}$	$\gamma_{da}$	$-iW_2^*$	$iW_2$	0	0	$-iW_1^*$	0	$-iW_4^*$	0	$iW_4$	0	$r_{aa}$	$\rho_{aa}$
0	$-\Gamma_{bb}-s$	$\gamma_{cb}$	$\gamma_{db}$	0	0	$-iW_5^*$	$iW_5$	$iW_1^*$	$iW_3$	0	0	$-iW_1^*$	0	$r_{bb}$	$\rho_{bb}$
0	0	$-\Gamma_{cc}-s$	$\gamma_{dc}$	$iW_2^*$	$-iW_2$	0	0	0	$-iW_3$	0	$-iW_6^*$	0	$iW_6$	$r_{cc}$	$\rho_{cc}$
0	0	0	$-\Gamma_{dd}-s$	0	0	$iW_5^*$	$-iW_5$	0	0	$iW_4^*$	$iW_6^*$	0	$-iW_4$	$r_{dd}$	$\rho_{dd}$
$-iW_2$	0	$iW_2$	0	$-i\Delta_{ac}-s$	0	0	0	$-iW_3$	0	$-iW_6^*$	0	$iW_1$	0	$r_{ac}$	$\rho_{ac}$
$iW_2^*$	0	$-iW_2^*$	0	0	$i\Delta_{ac}-s$	0	0	0	$-iW_1^*$	0	$-iW_4^*$	0	$iW_6$	$r_{ca}$	$\rho_{ca}$
0	$-iW_5$	0	$iW_5$	0	0	$-i\Delta_{bd}-s$	0	0	0	$iW_1^*$	$iW_3$	$-iW_4$	0	$r_{bd}$	$\rho_{bd}$
0	$iW_5^*$	0	$-iW_5^*$	0	0	0	$i\Delta_{bd}-s$	$iW_4^*$	$iW_6^*$	0	0	0	$-iW_1^*$	$r_{db}$	$\rho_{db}$
$-iW_1$	$iW_1$	0	0	$-iW_3^*$	0	0	$iW_4$	$-i\Delta_{ab}-s$	$iW_2$	$-iW_5^*$	0	0	0	$r_{ab}$	$\rho_{ab}$
0	$iW_3^*$	$-iW_3^*$	0	0	$-iW_1$	0	$iW_6$	$iW_2^*$	$i\Delta_{bc}-s$	0	$-iW_5^*$	0	0	$r_{cb}$	$\rho_{cb}$
$-iW_4$	0	0	$iW_4$	$-iW_6$	0	$iW_1$	0	$-iW_5$	0	$-i\Delta_{ad}-s$	$iW_2$	0	0	$r_{ad}$	$\rho_{ad}$
0	0	$-iW_6$	$iW_6$	0	$-iW_4$	$iW_3^*$	0	0	$-iW_5$	$iW_2^*$	$-i\Delta_{cd}-s$	0	0	$r_{cd}$	$\rho_{cd}$
$iW_1^*$	$-iW_1^*$	0	0	0	$iW_3$	$-iW_4^*$	0	0	0	0	0	$iW_5$	0	$r_{ba}$	$\rho_{ba}$
0	$-iW_3$	$iW_3$	0	$iW_1^*$	0	$-iW_6^*$	0	0	0	0	0	$-iW_5$	0	$r_{bc}$	$\rho_{bc}$
$iW_4^*$	0	0	$-iW_4^*$	0	$iW_6^*$	0	$-iW_1^*$	0	0	0	0	$i\Delta_{cd}-s$	$-iW_2^*$	$r_{da}$	$\rho_{da}$
0	0	$iW_6^*$	$-iW_6^*$	$iW_4^*$	0	0	$-iW_3$	0	0	0	0	$-iW_5^*$	$i\Delta_{cd}-s$	$r_{dc}$	$\rho_{dc}$

t=0

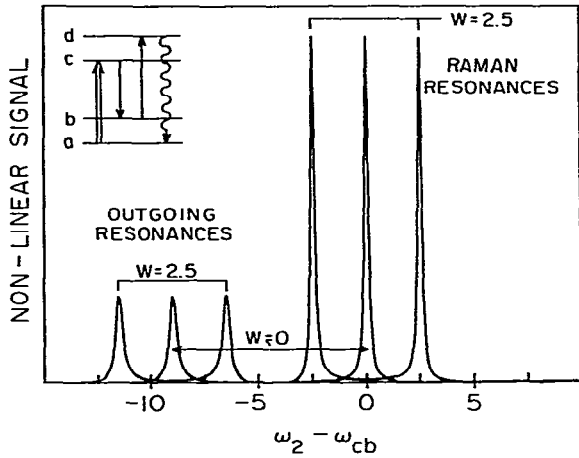


Fig. 8. Strong-field effect on the CARS resonance. The strong field is fixed on the  $a \rightarrow c$  transition. The four-level system is defined by the parameter values:  $\Gamma_{ab} = 0.1$ ,  $\Gamma_{ac} = 0.001$ ,  $\Gamma_{ad} = 0.2$ ,  $\Gamma_{bc} = 0.101$ ,  $\Gamma_{db} = 0.3$ ,  $\Gamma_{dc} = 0.201$ ,  $\gamma_{ba} = 0.2$ ,  $\gamma_{cb} = 0.001$  and  $\gamma_{ca} = 0.001$ . This choice corresponds to a situation encountered in pentacene ( $\nu' = 747 \text{ cm}^{-1}$ ,  $\nu = 756 \text{ cm}^{-1}$ ) under the assumption of pure radiative damping.

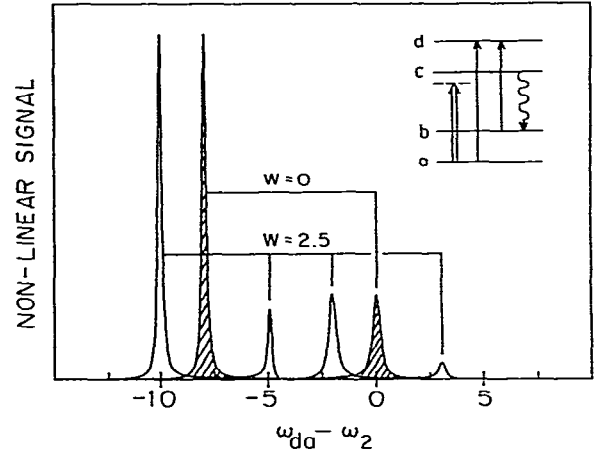


Fig. 9. Strong-field effect on the CSRS resonance. The same four-level model as in fig. 8 is used but with the fixed strong field detuned from the  $a \rightarrow c$  resonance by  $1 \text{ cm}^{-1}$ .

In the limit of all fields being weak the conventional CSRS susceptibility [11] is recovered in addition to the effects due to higher-order susceptibilities including one dependent on feeding given in eq. (81):

$$\chi_{\text{CSRS}}^{(3)} = -\mu_{ac}^* \mu_{ad} \mu_{bd}^* \mu_{bc} \left[ \frac{1}{\Delta_{ad} \Delta_{ab} \Delta_{bc}^*} + \frac{1}{\Delta_{ad} \Delta_{cd} \Delta_{bc}^*} - \frac{1}{\Delta_{ac}^* \Delta_{cd} \Delta_{bc}^*} \right]. \quad (80)$$

$$\chi_{\text{CSRS}}^{(5)} = (2\Gamma_{ac} \gamma_{cb} / \Gamma_{bb} \Gamma_{cc}) \mu_{ac}^2 \mu_{ac}^* \mu_{ad} \mu_{bd}^* \mu_{bc} / \Delta_{ac} \Delta_{ac}^* \Delta_{bc}^* \Delta_{bd}^* \Delta_{ab}. \quad (81)$$

Eq. (80) displays the three CSRS terms corresponding to the three diagrams that normally arise by means of an iterative solution of the density operator. This combination of three terms simplifies algebraically when all the pure dephasing effects vanish leading to resonances at  $\omega_4 - \omega_2 = \omega_{ba}$  and  $\omega_4 = \omega_{da}$ . In the presence of pure dephasing two additional resonances occur at  $\omega_4 - \omega_2 = \omega_{dc}$  and  $\omega_{cb} = 2\omega_2 - \omega_4$ . In the presence of a strong field, eq. (79) is the proper one to use and this has all four resonances as simulated in fig. 9. With increasing field strength of the strong field the resonances at  $\omega_{cb}$  and  $\omega_{dc}$  appear as power-induced extra resonances. The relative intensities of these four resonances are strongly dependent on the choice of the values for the feeding parameters, but the linewidths remain insensitive.

## 9. Conclusions

It was shown that the resonant non-linear response of certain multilevel systems can be calculated exactly (within the RWA) even when one of the incoming fields has unlimited strength. The non-perturbative approach that was developed allowed us to obtain explicit results for many common non-linear optical spectroscopic experiments. The method should have wide applicability, and even in the case all the fields are weak provides a rapid system for generating the formulas usually obtained by iterative solution of the Liouville equation.

A number of important new results is obtained from the exact approach: In the presence of a strong field the

dynamical parameters of the system that determine the response are more clearly evaluated than in the weak-field case, whenever the weak field is scanned. Scanning the strong field yields information mainly about the light source. The extra resonances that are usually assumed to occur only in the presence of pure dephasing processes in the medium, are seen to occur by virtue of the finite strength of the strong field. Exact (RWA) formulas for the CARS and CSRS in four-level systems are given.

The method developed in this paper can be applied to a variety of experimental situations including CARS and CSRS, as mentioned above, polarization spectroscopy, other four-wave resonant processes, "second-order" processes such as sum- and difference-frequency generation in three-level systems. Other situations such as four-wave mixing in two- and three-level schemes can be evaluated using the present techniques applied in a stepwise manner.

### Acknowledgement

We are indebted to Professor Karl Freed for valuable suggestions concerning the applicability of the method of ref. [7] to non-linear optical problems.

### Appendix A

In this appendix it is shown that the operator  $\hat{X}$ , corresponding to the matrix  $\mathbf{X}$  defined in eq. (26), has the form:

$$\hat{X} = i(\hat{A} + \hat{\tilde{L}} - i\hat{\Gamma}) , \quad (\text{A1})$$

where  $\hat{X}$ ,  $\hat{A}$ ,  $\hat{\tilde{L}}$  and  $\hat{\Gamma}$  are superoperators. The matrix elements of  $\hat{X}$  are shown to be given by:

$$\hat{X}_{\mu\nu,\alpha\beta} = -i\Delta_{\mu\nu}\delta_{\mu\alpha}\delta_{\nu\beta} + \gamma_{\beta\mu}\delta_{\mu\nu}\delta_{\alpha\beta} + i\delta_{\nu\beta}W_j(\mu \leftarrow \alpha) - i\delta_{\mu\alpha}W_k(\beta \leftarrow \nu) . \quad (\text{A2})$$

According to their usual definitions [23–25] superoperators,  $\hat{A}$ , act on operators,  $\rho$ , according to the prescription

$$(\hat{A}\rho)_{\mu\nu} = \sum_{\alpha\beta} A_{\mu\nu,\alpha\beta} \rho_{\alpha\beta} .$$

The product of two superoperators is defined as

$$(\hat{A}\hat{B})_{\mu\nu,\alpha\beta} = \sum_{\sigma\tau} A_{\mu\nu,\sigma\tau} B_{\sigma\tau,\alpha\beta} .$$

The unitary transformation defined through eq. (14) can be written as a superoperator  $\hat{U}$ , so that

$$\tilde{\rho} = \hat{U}\rho , \quad (\text{A3})$$

with

$$\hat{U}_{\mu\nu,\alpha\beta} = \delta_{\mu\alpha}\delta_{\nu\beta} \exp[i(A_\mu - A_\nu)t] .$$

It follows that  $\hat{\tilde{U}}$  has the form  $i\hat{A}\hat{U}$ , with  $\hat{A}$  given by

$$\hat{A}_{\mu\nu,\alpha\beta} = \delta_{\mu\alpha}\delta_{\nu\beta}(A_\mu - A_\nu) = \delta_{\mu\alpha}\delta_{\nu\beta}s_{\mu\nu}\omega_j . \quad (\text{A4})$$

Having found  $\hat{\tilde{U}}$ , the equation of motion for  $\rho$  can be found in the required form from eq. (A3):

$$\dot{\tilde{\rho}} = \hat{\tilde{U}}\dot{\rho} + \dot{\hat{\tilde{U}}}\rho = i\hat{A}\hat{U}\rho + \hat{U}(i\hat{\tilde{L}} + \hat{\Gamma})\rho .$$

Therefore

$$\dot{\tilde{\rho}} = (i\hat{A} + i\hat{\tilde{L}} + \hat{\Gamma})\tilde{\rho} = \hat{X}\tilde{\rho} , \quad (\text{A5})$$

where the transformed Liouville operator  $\tilde{\mathcal{L}} = \hat{U}\hat{\mathcal{L}}\hat{U}^{-1}$ . The matrix elements of  $\hat{X}$  now follow from the definitions of the superoperator elements (A4) along with

$$\tilde{\mathcal{L}}_{\mu\nu,\alpha\beta} = \omega_{\nu\mu}\delta_{\mu\alpha}\delta_{\nu\beta} + \delta_{\nu\beta}(\mathbf{\mu}_{\mu\alpha} \cdot \mathbf{e}_j)\epsilon_j - \delta_{\mu\alpha}(\mathbf{\mu}_{\beta\nu} \cdot \mathbf{e}_k)\epsilon_k$$

and

$$\hat{\Gamma}_{\mu\nu,\alpha\beta} = -\Gamma_{\mu\nu}\delta_{\mu\alpha}\delta_{\nu\beta} + \gamma_{\beta\mu}\delta_{\mu\nu}\delta_{\alpha\beta} = \tilde{\Gamma}_{\mu\nu,\alpha\beta}.$$

## Appendix B

To prove that the superoperator matrix  $\mathbf{X}$  cannot be inverted and hence eq. (23) has a non-trivial solution, let us sum the rows of  $\mathbf{X}$  corresponding to the diagonal elements of  $\hat{\rho}$ . This yields a vector  $Z$  with elements

$$\begin{aligned} Z_{\sigma\tau} &= \sum_{\mu} \hat{X}_{\mu\mu,\sigma\tau} \\ &= \sum_{\mu} [-\Gamma_{\mu\mu}\delta_{\mu\sigma}\delta_{\mu\tau} + \gamma_{\mu\tau}\delta_{\sigma\tau} + i\delta_{\mu\tau}W(\mu \leftarrow \sigma) - i\delta_{\mu\sigma}W(\tau \leftarrow \mu)] \\ &= \delta_{\sigma\tau} \left[ \sum_{\mu} \gamma_{\mu\tau} - \Gamma_{\mu\mu} \right] = 0, \end{aligned}$$

where we have used eq. (5) in the last step.

## References

- [1] R.M. Hochstrasser and H.P. Trommsdorff, *Accounts Chem. Res.*, to be published.
- [2] S.Y. Yee, T.K. Gustafson, S.A.J. Druet and J.-P.E. Taran, *Opt. Commun.* 23 (1977) 1.
- [3] T.K. Yee and T.K. Gustafson, *Phys. Rev. A* 18 (1978) 1597.
- [4] J.-L. Oudar and Y.R. Shen, *Phys. Rev. A* 22 (1980) 1141.
- [5] N.F. Ramsay, *Molecular beams* (Oxford Univ. Press, London, 1956);  
J.C. McGurk, T.K. Schmalz and W.H. Flygare, *Advan. Chem. Phys.* 25 (1974) 1.
- [6] L.R. Wilcox and W.E. Lamb Jr., *Phys. Rev.* 119 (1960) 1915.
- [7] K.F. Freed, *J. Chem. Phys.* 43 (1965) 1113.
- [8] C. Wiemann and T.W. Hänsch, *Phys. Rev. Letters* 36 (1976) 1170.
- [9] N. Bloembergen, H. Lotem and R.T. Lynch Jr., *Indian J. Appl. Chem.* 16 (1978) 151.
- [10] P.L. DeCola, J.R. Andrews, R.M. Hochstrasser and H.P. Trommsdorff, *J. Chem. Phys.* 73 (1980) 4695.
- [11] J.R. Andrews, R.M. Hochstrasser and H.P. Trommsdorff, *Chem. Phys.* 62 (1981) 87.
- [12] J.R. Andrews and R.M. Hochstrasser, *Chem. Phys. Letters* 82 (1981) 381; 83 (1981) 427.
- [13] T. Yajima, *Opt. Commun.* 14 (1975) 378.
- [14] T. Yajima, H. Souma and Y. Ishida, *Opt. Commun.* 18 (1976) 150.
- [15] T. Yajima and H. Souma, *Phys. Rev. A* 17 (1978) 309.
- [16] T. Yajima, H. Souma and Y. Ishida, *Phys. Rev. A* 17 (1978) 224.
- [17] H. Souma, E.J. Heilweil and R.M. Hochstrasser, *J. Chem. Phys.* 76 (1982) 5693.
- [18] J.R. Andrews and R.M. Hochstrasser, *Chem. Phys. Letters* 76 (1980) 207, 213;  
H.J. Heilweil, R.M. Hochstrasser and H. Souma, *Opt. Commun.* 35 (1980) 227.
- [19] Y. Prior, A.R. Bodgan, M. Dagenais and N. Bloembergen, *Phys. Rev. Letters* 46 (1981) 111.
- [20] N. Bloembergen, *Nonlinear optics* (Benjamin, New York, 1965).
- [21] N. Bloembergen and Y.R. Shen, *Phys. Rev.* 133A (1964) 37.
- [22] B. Dick and R.M. Hochstrasser, *J. Chem. Phys.* 78 (1983), to be published.
- [23] J.A. Crawford, *Nuovo Cimento* 10 (1958) 698.
- [24] H. Primas, *Helv. Phys. Acta* 34 (1961) 345.
- [25] K. Lendi, *Chem. Phys.* 20 (1977) 135.